Hindawi
Advances in Materials Science and Engineering
Volume 2022, Article ID 2839150, 10 pages
https://doi.org/10.1155/2022/2839150

Research Article

Impact of Silicon Carbide Particles Weight Percentage on the Microstructure, Mechanical Behaviour, and Fractography of Al2014 Alloy Composites

H. S. Vasanth Kumar,[1] K. Revanna,[2] Nithin Kumar,[3] N. Sathyanarayana,[1] N. Madeva,[4] G. A. Manjunath,[5] and H. Adisu[6]

[1]*Department of Mechanical Engineering, Government Engineering College, Kushalnagar 571234, Karnataka, India*
[2]*Department of Mechanical Engineering, Government Engineering College, Chamarajanagara 571313, Karnataka, India*
[3]*Department of Mechanical Engineering, NMAM Institute of Technology, Nitte 574110, Karnataka, India*
[4]*Aircraft Research and Design Centre, HAL, Bangalore 560037, Karnataka, India*
[5]*Department of Mechanical Engineering, KLS Gogte Institute of Technology, Belagavi 590006, Karnataka, India*
[6]*Department of Mechanical Engineering, WOLLO University, Kombolcha Institute of Technology, Kombolcha, Ethiopia*

Correspondence should be addressed to H. Adisu; adisu.haile@wu.edu.et

Received 18 June 2022; Revised 6 July 2022; Accepted 3 August 2022; Published 25 August 2022

Academic Editor: Temel Varol

The microstructure, mechanical characteristics, and tensile fractography of Al2014 alloy reinforced composites with 5 and 10% wt. % of 150 to 160 micron-sized SiC particles were investigated in this study. The melt stir process was used to make composites comprising 5 and 10% SiC particles in the Al2014 alloy. To increase the wettability between Al matrix SiC particles, SiC particles were warmed to 300 degrees Celsius before being disseminated into the Al2014 alloy matrix in two phases. SEM, EDS, and XRD were used to examine the specimens micro-structurally. ASTM standards were used to evaluate the mechanical characteristics of micro SiC particles reinforced Al alloy composites with a content of 5 to 10%. SEM and EDS microstructural tests revealed the existence and dissemination of micro SiC particles in the Al2014 matrix. The addition of 5 and 10% weight % of micro SiC particles to Al2014 alloy improved its hardness, ultimate, yield, and compression strength. With the addition of 10 wt. % of SiC, the hardness, ultimate strength, yield strength, and compression strength of Al2014 alloy improved to 15.96%, 35.2%, 43.8%, and 38.7%, respectively. Furthermore, the presence of SiC particles reduced the ductility of Al2014 alloy. SEM microphotographs were used to examine the manufactured Al2014 with SiC composites for tensile fracture analysis, revealing the various mechanisms intricate in tensile fracture.

1. Introduction

A composite material can be defined as a combination of more than one identifiable constituent intentionally combined to obtain homogeneous structures with better properties than individual used alone [1, 2]. In contrast to metallic alloys, the constituents of the composites retain their mechanical, physical, and chemical properties. The strength and stiffness of the composite is provided by the reinforcing phase. In most of the cases, the reinforcement employed in composites is stronger, stiffer, and harder than the matrix and it can be in the form of a fibre or a particulate [3, 4]. The dimensions of the particulates used in composites are more or less equal in all the directions. Particulates may be of spherical, platelets, or of any other regular or irregular geometry. Continuous fibre composites tend to be much stronger and stiffer than particulate composites. Because of the difficulties in processing and increasing brittleness, particulate composites contain less reinforcement which makes them much cheaper and are referred as discontinuously reinforced MMCs [5, 6].

Further, particulate-reinforced composites are isotropic in nature when compared to fibre-reinforced composites

and offer higher ductility which makes them an attractive alternate to the conventional metals. From a practical point of view, chemical compatibility among the matrix and reinforcement is of high significance. It is required to retain the separate identity of the matrix and reinforcement during their exposure to extreme processing temperatures and applications [7]. To achieve thermal compatibility, understanding and controlling of extensive chemical reactions between the reinforcement and matrix within a bound are necessary. Nonthermal compatibility between them results in degradation of mechanical and thermal properties. During cooling of composites from their processing and forming temperatures, due to the large difference in coefficient of thermal expansion between the matrix and reinforcement, residual stresses and deformations gets introduced. These residual stresses and deformations can also be introduced during their applications at higher temperatures which could be deleterious. Both strength and stiffness also depend on the type of reinforcing element and their orientation in the matrix [8]. Continuous fibres possess large aspect ratios and normally have a preferred orientation. On the other hand, discontinuous fibres have small aspect ratios and generally oriented in random directions. Out of all the properties, the directionality is possibly the prime characteristic that differentiates the fibre-reinforced composites from the conventional metals/particulate composites.

In aerospace and automotive applications, hybrid composites with better mechanical and chemical characteristics are frequently employed. Because of their inexpensive cost, aluminium hybrid MMC are commonly made and employed in structural applications [9, 10]. Following that, much study has been done in AMC with the addition of reinforcements to aluminium such as B_4C, Al_2O_3, SiC, and fly ash, among others [11, 12]. The purpose of this analysis was to highlight the most recent advancements in AMCs as well as the impact of reinforcements [13]. The impact of aluminium matrix composite mechanical and tribological behaviour has been discussed. The Al2014 alloy was chosen for this investigation because it is readily accessible commercially and is frequently utilized for structural purposes in the manufacturing industry. A lot of research has been done on adding B_4C, Al_2O_3, SiC, and fly ash to improve hardness, tensile, YS, wear resistance, machinability, good abrasion resistance, stiffness-to-weight ratios, strength-weight ratios, and enhanced high temperature performance as shown in the current work [14, 15]. The current study looks at how to make (fabricate) these sophisticated engineered materials via stir casting. The mechanical behavior of composites will increase as the amount of SiC rises. It was also discovered that when the particle size increased, the wear rate reduced at a fixed volume fraction. The addition of SiC to aluminium improves composites' wear resistance [16]. It also demonstrates that higher operating temperatures result in increased specific strength, stiffness, and wear resistance [17, 18].

MMCs are produced by various manufacturing processes which are typically classified on the basis of their processing temperature. Of course, the method of introducing reinforcement into given matrix is generally specified by the type of reinforcement, particle size, and morphology of the reinforcement [19]. Fabrication of MMCs in the liquid state is generally done by a stir casting route due to its reliability and lower cost [20]. Seo and Kong [21] noted that this method is simple, flexible, and most suitable for production in large quantity. Naher et al. [22] showed that the cost of preparing composites by the casting method is just 30–50% of the other competing methods.

Using 150 to 160 micron-sized SiC particles in an Al2014 alloy matrix, a limited research was carried out based on the available literature. Stir casting was used to create Al2014 alloy metal composites with SiC particles. To avoid agglomeration, SiC added to the aluminium melt in two stages, instead of adding SiC particles in one time into the melt; in the present study, a novel two step stir casting method is adopted. After that, the manufactured aluminium matrix composites are put through a series of mechanical tests.

2. Experimental Details

2.1. Materials Used. Al2014 is a wrought alloy with copper as the principal alloying element, which has a melting point of 660°C and a density of 2.80 g/cm^3. The Al2014 alloy is primarily used in aerospace and transportation applications. Al2014 offers excellent toughness, corrosion resistance, and higher temperature strength, as well as a strong self-healing capacity throughout the welding process. Table 1 displays the chemistry of Al2014.

The silicon carbide reinforcing material from Bioaid Scientific Industries Ltd., Bangalore, is 150 to 160 μm in size. The reinforcement material is black in hue. The density of the reinforcement particle is 3.10 g/cm^3 [23], with a melting point of 3200°C and a hardness of 3100–3150 kg/mm^2. The SEM and EDS of SiC utilized to make the composites are shown in Figures 1 and 2.

2.2. Methodology and Testing. The Al2014-SiC composites are made using the stir casting process. In a graphite crucible, a measured amount of Al2014 alloy is put. After that, the crucible is positioned in the electric furnace. To melt the Al2014 alloy, the furnace is kept at 750 degrees Celsius. Simultaneously, SiC particles are roasted to 300°C in a separate oven to eliminate moisture content and promote wettability. Hexochlorthane, a degassing agent, is given to the molten metal to prevent undesirable gases from escaping. A unique two-step reinforcement addition approach is used to pour a known quantity of SiC particles into molten metal. The casting is then mixed homogeneously using a mechanical stirrer made of a zirconium-coated material at 300 rpm for 5 minutes. The molten metal is put into the mould die right away. Cast iron is used to make the die. The cast iron die has a length of 120 mm and a dia. of 15 mm. The procedure is repetitive for SiC particles reinforced composites with 10% SiC. To perform the needed testing, the castings are machined according to ASTM standards. The stir casting setup utilized to make the Al2014–SiC composites is shown in Figure 3. Figure 4 shows the composites that were prepared for the study.

Table 1: Chemistry of Al2014 alloy.

Elements	Si	Fe	Cu	Mg	Zr	Zn	Cr	Mn	Al
Weight (%)	0.7	0.5	5.0	0.3	0.20	0.1	0.10	0.4	Bal

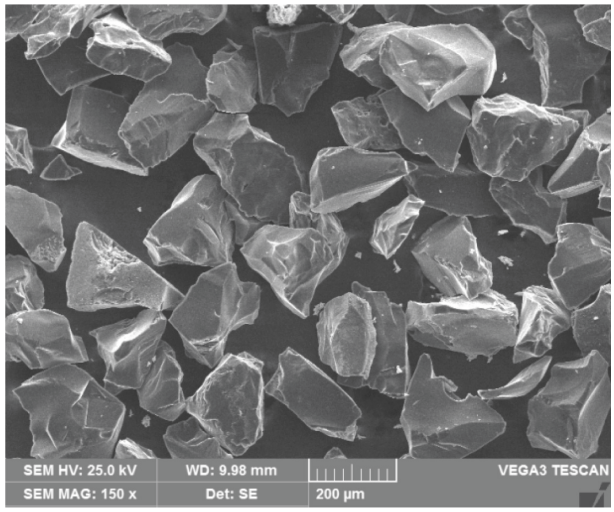

Figure 1: SEM micrograph of SiC particles.

The specimen is arranged for microstructural analysis after casting to determine the uniform circulation of SiC reinforcement in the Al2014 alloy. Microstructure pictures of Al2014 alloy and Al2014 alloy SiC composites are taken. Microstructure specimen dimensions are 10 mm in dia., and 5 mm in height. 300, 600, and 1000 grit paper are used to grind the specimen's surface. The surface is then polished with a polishing paper for a smoother finish. Following that, the samples are cleaned with distilled water to eliminate any foreign particles such as dirt or other contaminants that may have accumulated on the polished surface. Keller's reagent [24] is used to etch the specimens to create a contrast surface.

The specimen is machined according to ASTM standard E10 [25] for the hardness test. The Brinell hardness tester is used to test the hardness. The polished surface of the specimen is smooth. A 5 mm ball depression is made on the specimen, which is then loaded with 250 kg. On the surface of the material, three indentation marks are made and the consequences are analysed.

The density measurement is based on the existence of porosity in the sample. The rule of mixture is used to determine theoretical values for the base and Al2014-SiC composites. The ASTM D290 [26] method is used to determine the experimental density values using the Archimedean method.

To investigate the tensile strength of Al2014 alloy and SiC composites, the samples are machined according to ASTM standard E8 [27]. Three samples are taken for the tensile test to ensure precise results. The computerized tensile machine is used to determine tensile strength, examine the effect of even dissemination, and investigate the behavior of Al2014–SiC composites under unidirectional tension. The sample has an overall length of 104 mm, a gauge length of 45 mm, and a gauge dia., of 9 mm. The mechanical presentation of cast alloys and composites can be examined using this tensile test to determine ultimate, yield, and elongation. The tensile sample is shown in Figure 5. The compression strength of Al2014 alloy and its SiC reinforced composites are evaluated as per ASTM E9 standard [27].

3. Results and Discussion

3.1. Microstructural Studies. Scanning electron microphotographs of Al2014 alloy reinforced composites with 5 and 10% SiC particles are shown in Figure 6(a)–6(c). The SEM picture of Al2014 alloy is shown in Figure 6(a). This indicates the absence of particles and the presence of clean grain boundaries. There are no voids or other casting flaws visible on the microscope. Microphotographs of Al2014-5 wt. % SiC and Al2014-10 wt. % SiC composites are shown in Figures 6(b) and 6(c), respectively. The SiC particles, which are noticeable in the micrographs, are present in 5 and 10% of SiC strengthened composites, according to the micrographs. Because of the revolutionary 2-step stir casting technique used to create the composites, these particles are devoid of agglomeration. Furthermore, the microstructure surface of Al2014-10 wt. % SiC composites comprises a greater number of SiC particles, which are spread throughout the matrix Al2014 alloy.

The EDS spectra of Al2014 alloy with 10% SiC particles composites are shown in Figure 7(a) and 7(b). Cu is the predominant alloying element in Al2014 alloy, which also comprises Si, Fe, and Mg, as shown in Figure 7(a). The EDS spectrum of Al2014-10 wt. percent SiC particles composites is also shown in Figure 7(b). The attendance of SiC in the Al2014 in the form of Si and C elements was visible in the EDS spectrum of composites. The existence of Si and C elements, as well as Cu, Mg and Fe elements, validates the integrity of the composites casting approach.

The Al2014 and Al2014-10 wt. percent SiC composites are analysed using an x-ray diffractometer (PANalytical, Netherland-made). The XRD pattern of Al2014 is given in Figure 8(a); typically, aluminium phases are existing at various peaks, as seen in Figure 8(a). At 39°, 45°, 65°, and 79°, the incidence of Al phases is established with varying intensities. At 39°, the Al phase has the highest intensity. The XRD pattern of Al2014-10 wt. percent SiC composites is shown in Figure 8(b). Figure 8(b) shows the different phases, such as Al and SiC. As previously stated, Al phases are generally available at various 2 theta angles with varying intensities; while SiC particle phases can be found at 36°, 60°, and 71° degrees with varying intensities. The presence of silicon carbide particles in the Al2014 alloy has been found in the form of SiC phases.

3.2. Density Measurements. Figure 9 shows the densities of Al2014 alloy, Al2014 with 5 and 10 wt. percent SiC particles reinforced composites. The rule of mixture is used to calculate the theoretical densities of Al2014 and SiC reinforced composites. Furthermore, experimental densities are calculated using the Archimedean principle. Al2014 has a theoretical density of 2.80 g/cm^3, but SiC particles employed in the study have a density of 3.10 g/cm^3. The density of the

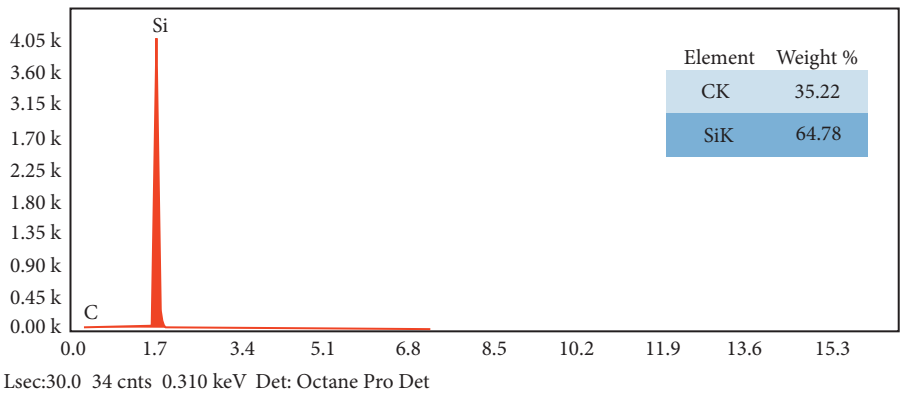

Figure 2: EDS spectrum of SiC particles.

Figure 3: Stir casting setup (courtesy: PES College Of Engineering, Mandya).

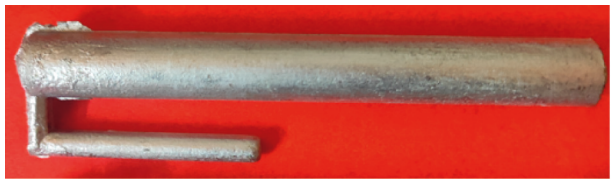

Figure 4: Al2014-SiC composite after casting.

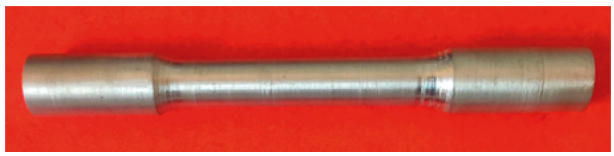

Figure 5: Tensile test specimen.

base alloy has grown from 2.80 g/cm^3 to 2.827 g/cm^3 as the weight % of SiC particles in the Al2014 matrix increases from 5 to 10 wt. percent. The higher density of SiC particles in contrast to Al matrix accounts for the increased density with SiC particle integration. The reinforced particles higher density improves the matrix alloy's overall density. Furthermore, as seen in the graph, the experimental densities are slightly lower than the theoretical densities, and the difference amongst the two is tiny. The expected density of the Al2014 matrix is 2.80 g/cm^3, whereas the observed density is 2.732 g/cm^3, highlighting the importance of the composites' casting procedure.

3.3. Hardness Measurements. Figure 10 shows the hardness of Al2014 alloy, Al2014-5, and 10 wt. % of SiC composites. The plot shows that the hardness of Al2014 increases when the percentage of SiC particles increases from 5 to 10%. The hardness of the alloy as cast is 70.2 BHN, while it is 81.7 BHN and 97.4 BHN after including 5 and 10 wt. percent SiC, respectively. The hardness of Al2014 alloy-10 wt. % SiC composites increased by 38.7%. The existence of hard SiC in the ductile matrix improves the hardness of Al2014 alloy. SiC particles have a hardness of 3150 BHN, so incorporating such a high-hardness substantial into a soft Al material helps to improve hardness. Furthermore, the dislocation density is created by the thermal co-efficient mismatch among the Al2014 alloy and SiC particles, resulting in greater strain hardening in the composites. The composites hardness is increased through the strain hardening phenomenon [28, 29]. Basically reinforcements are more rigid and stronger than the Al2014 alloy matrix and these strengthening particles always try to avoid plastic deformation.

3.4. Ultimate Tensile and Yield Strength. Figure 11 depicts the effect of SiC particles on the strength of Al2014 alloy. The strength of the Al2014 alloy has increased as the weight percent of SiC increases in the soft Al matrix as shown in Figure 11. The Al2014 alloy's ultimate tensile strength is 194.4 MPa. In addition, the UTS of Al2014-5 wt. % SiC and Al2014-10 wt. % SiC composites are 224.5 MPa and 262.4 MPa, respectively. After incorporating 10% weight percent of 150 to 160 micron-sized SiC particles into Al2014 alloy, the UTS improved by 35%.

Figure 12 depicts the effect of SiC content on the yield strength of the Al2014 alloy. The strength of the Al2014 alloy has increased as the weight percent of SiC content increases

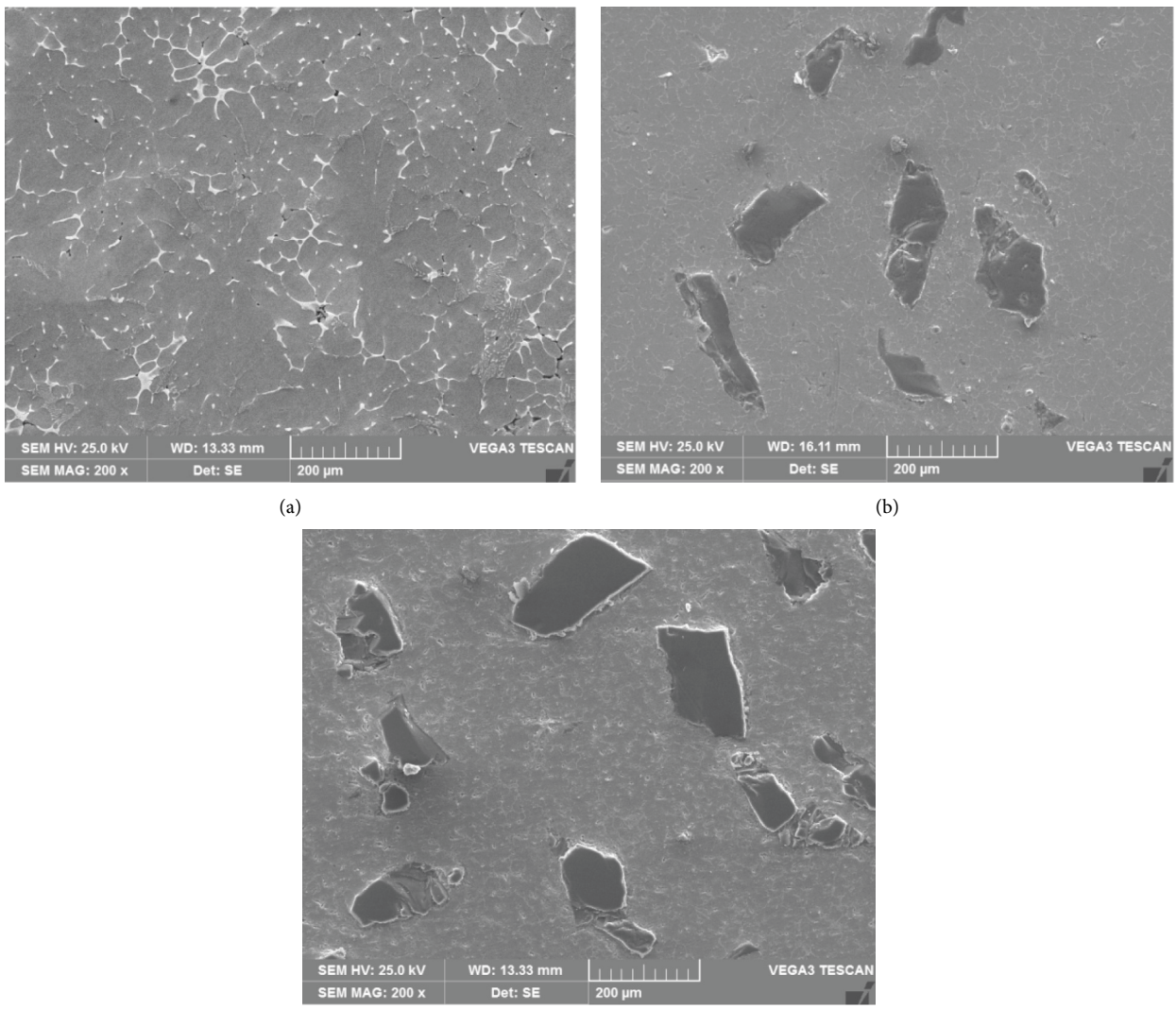

Figure 6: SEM microphotographs of (a) Al2014 alloy, (b) Al2014-5 wt. % of SiC, and (c) Al2014-10 wt. % of SiC composites.

in the soft Al matrix as shown in Figure 12. The Al2014 alloy has a yield strength of 161.5 MPa. In addition, the YS of Al2014-5 wt. % SiC and Al2014-10 wt. % SiC composites are 201.2 MPa and 232.1 MPa, respectively. After incorporating 10% weight percent of 150 to 160 micron-sized SiC particles into the Al2014 alloy, the YS improved by 43.7 percent.

The strength of Al2014 was increased with 5 and 10% wt. % of tiny SiC particles, as shown in plots 11 and 12. The existence of the SiC element in the matrix increases the strength of Al alloy. The hard elements make the soft matrix brittle, allowing it to withstand higher directed loads. These hard particles operate as load-bearing elements in composites, enhancing the composites' strength. Furthermore, according to the Hall–Petch strengthening process [30], the insertion of microparticles in the Al matrix reduces the grain size of the composites, which contributes to the material's increased strength [31]. The temperature mismatch among the Al2014 and the SiC particles is large, resulting in density dislocations according to the Orowan principle [32]. The formation of density dislocations causes strain strengthening within the Al-SiC melt, resulting in increased strength.

3.5. Percentage Elongation. The ductility of the Al2014 alloy and Al2014 alloy with 5 and 10% micro-SiC composites is shown in Figure 13. The plot shows that ductility diminishes as the amount of SiC in the matrix increases. The decrease in ductility is due to the presence of hard SiC in the matrix; however, the intense multidirectional stresses at the Al2014 alloy SiC contact prevent further material elongation. There is a strong connection between Al and SiC particles, as well as the efficient transfer of applied load to a larger number of tiny SiC particles. As a result of these possessions, the elongation obtained in Al2014 alloy–10% SiC composites is lower than that obtained in base amalgam and 5% SiC particles reinforced composites.

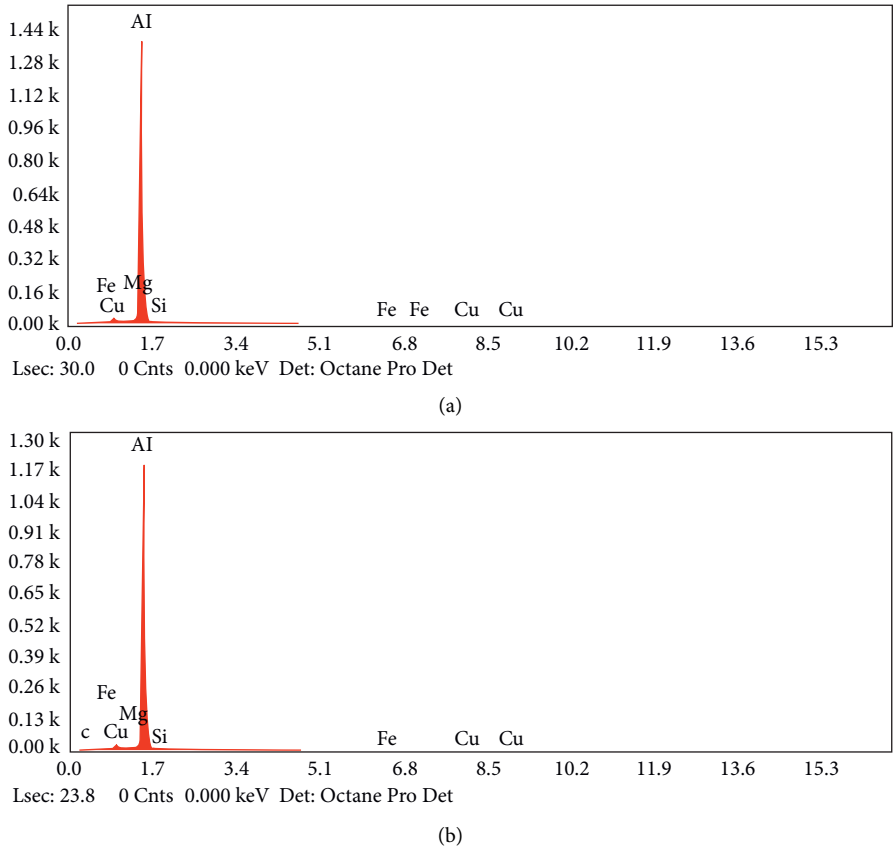

Figure 7: EDS spectrum of (a) Al2014 alloy and (b) Al2014-10 wt. % of SiC composites.

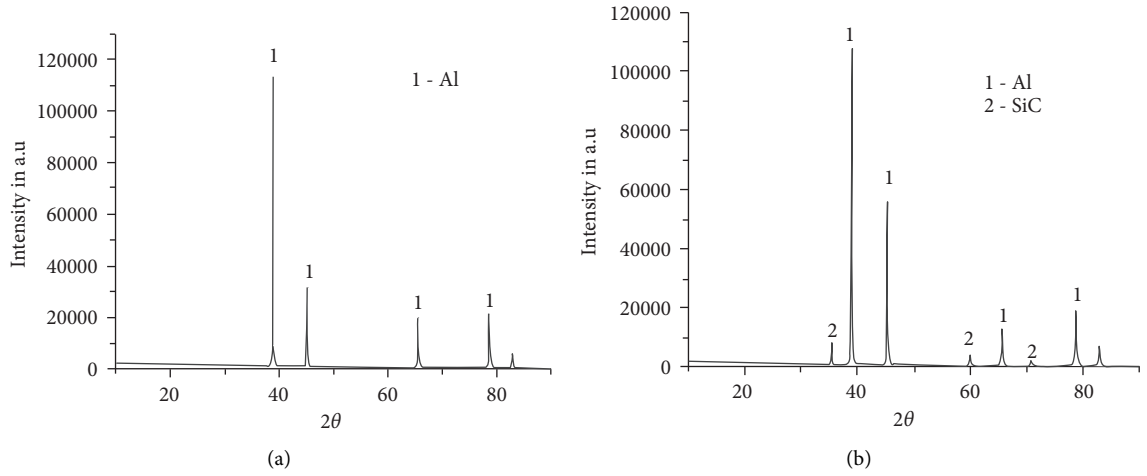

Figure 8: XRD patterns of (a) Al2014 alloy and (b) Al2014-10 wt. % of SiC composites.

3.6. Compression Strength. Figure 14 shows the compression strength of Al2014 and Al2014 with 5 and 10% SiC composites. The incidence of hard particle phase boosted the compressive strength of the Al2014 matrix, which rose further as the wt. % of SiC increased, according to the plot. Because these ceramics are tougher in nature, compressive strength is always used to determine the strength of the carbide or oxide particles. The large quantity of grain refinement produced with the inclusion of SiC particles, the presence of evenly distributed tougher components, and dislocation formed due to the modulus discrepancy and thermal expansion co-efficient can all be contributed to the Al-SiC composites' strength [33]. According to the results of Figure 14, the effect of SiC content on compressive strength is significant. This validates the clear effect of SiC on Al-SiC composites' strength.

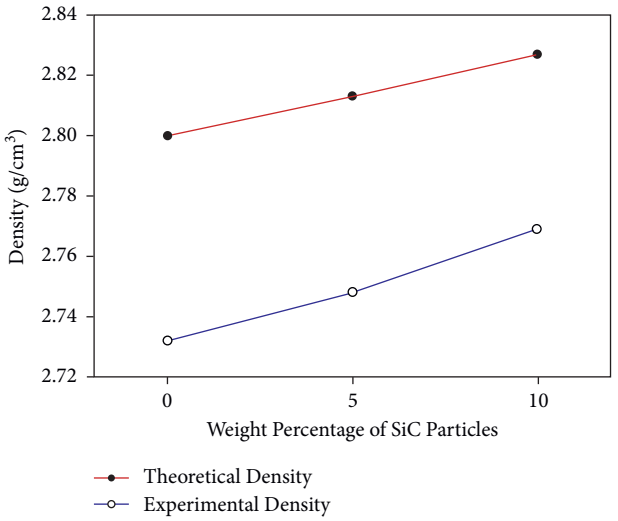

Figure 9: Theoretical and experimental densities of Al2014–SiC composites.

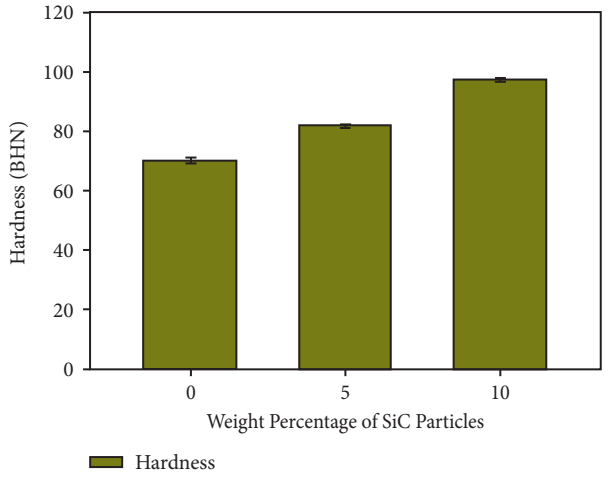

Figure 10: Hardness of Al2014 alloy and SiC composites.

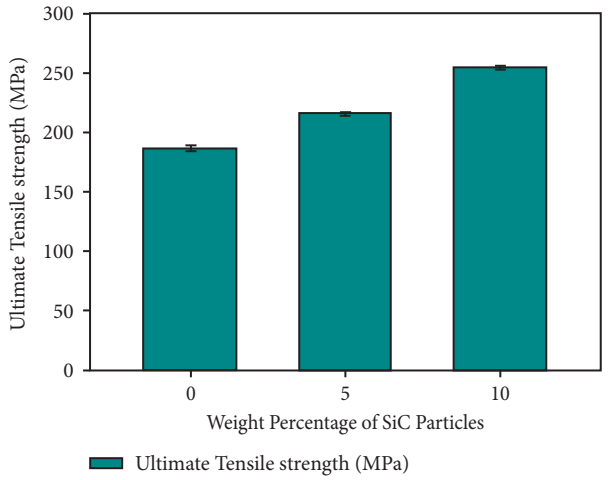

Figure 11: Ultimate strength of the Al2014 alloy and SiC composites.

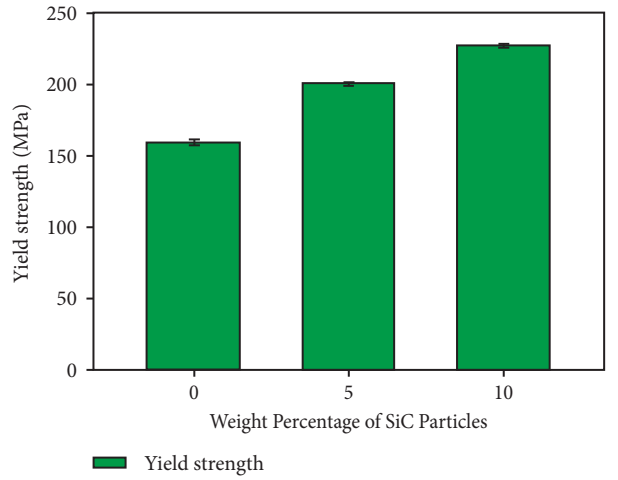

Figure 12: Yield strength of the Al2014 alloy and SiC composites.

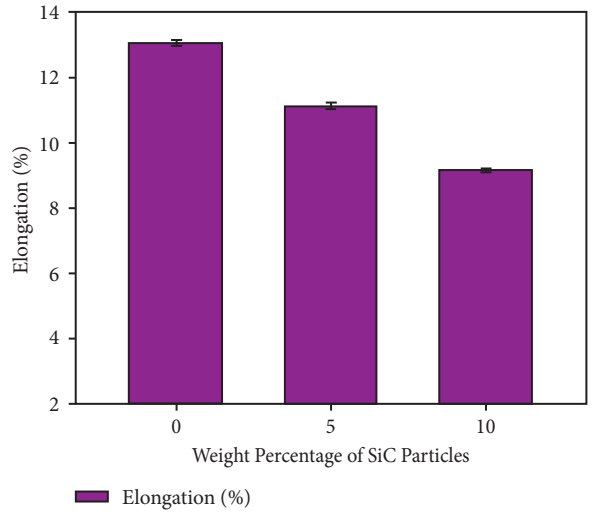

Figure 13: Ductility of the Al2014 alloy and SiC composites.

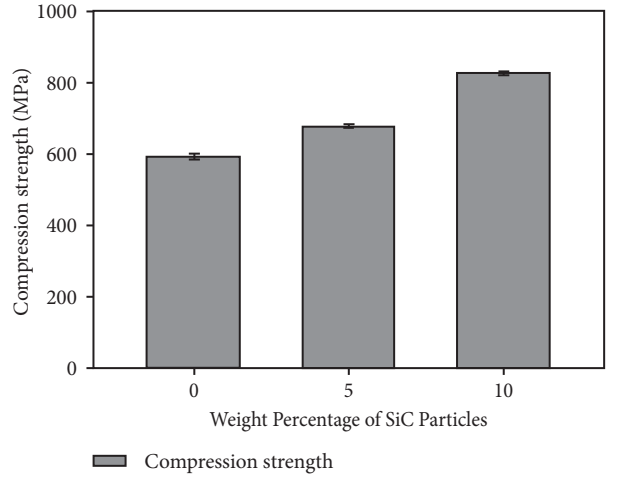

Figure 14: Compression strength of the Al2014 alloy and SiC composites.

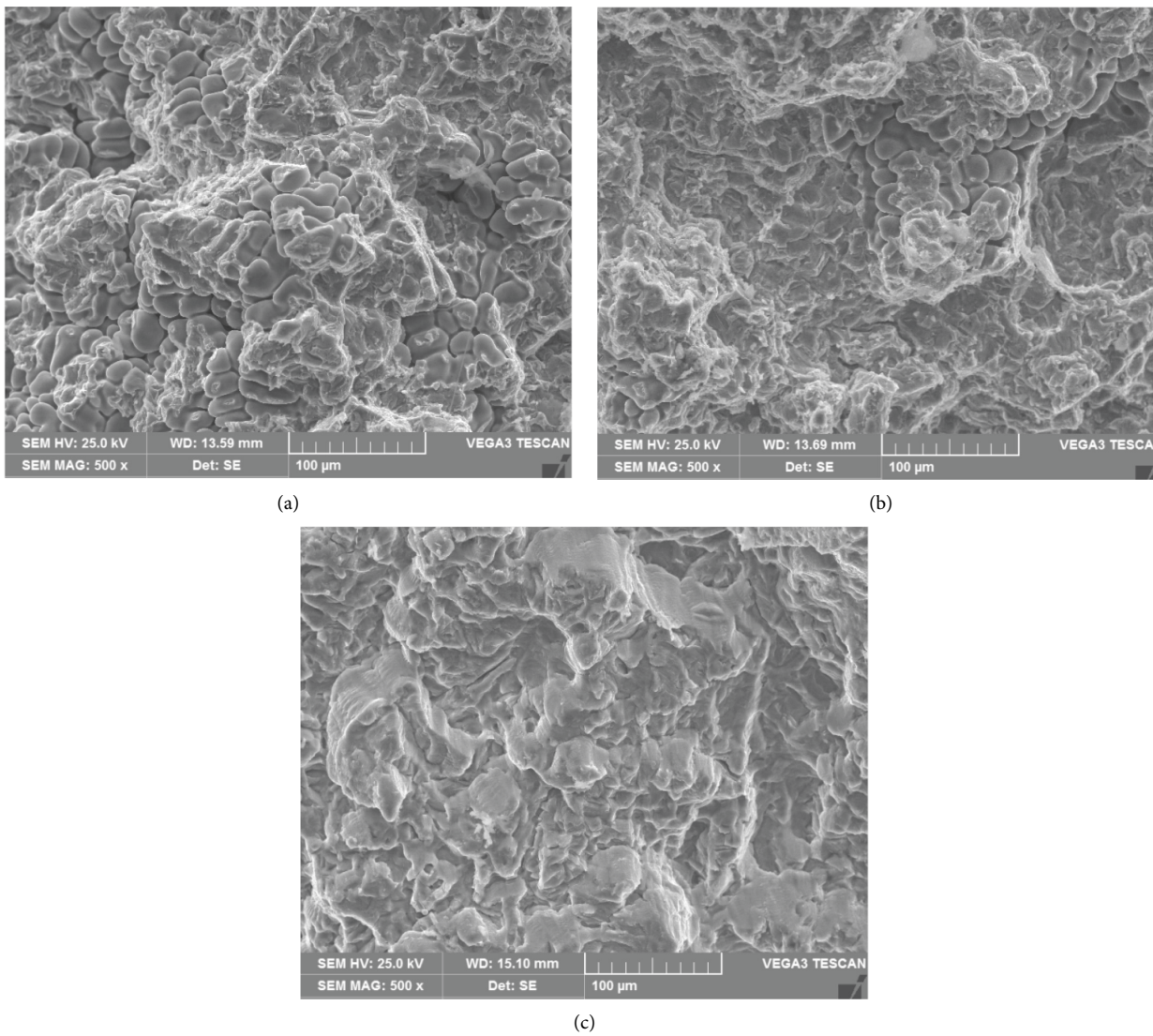

Figure 15: Tensile fractured surfaces SEM images of (a) Al2014 alloy, (b) Al2014-5 wt. % SiC, and (c) Al2014-10 wt. % SiC composites.

3.7. Tensile Fractography. SEM pictures of the fractured areas of Al2014 and Al2014 with 5 and 10% SiC composites are shown in Figure 15(a)–15(c). The excellent bonding among the matrix and the SiC reinforcement can be inferred from all of the tension fractured micrographs. In Figure 15(a), the shattered surface of 500x magnification pictures of Al2014 alloy is shown. The ductile fracture is shown by the fractured surface of the as cast alloy, which has visible grains.

The cracked surfaces of Al2014-5 wt. % SiC and Al2014-10 wt. % SiC composites are shown in Figure 15(b) and 15(c). According to the micrographs, the composites become more brittle as the SiC reinforcement increases. The fractured surface of Al2014-10 wt. % of SiC composites demonstrates this increased brittleness. Furthermore, the brittle fracture is directly connected to the composites' elongation [34]. The ductility of the composites decreases as the weight percent of SiC increases, as discussed in the percentage elongation section.

4. Conclusions

The Al2014–SiC metal composites were successfully produced using the metallurgical process and the stir casting method. SEM/EDS and XRD patterns were used to examine the microstructural characteristics of the produced Al20214 alloy and Al2014 with 5 and 10% SiC composites. SEM micrographs, EDS analysis, and XRD patterns were used to show the distribution and existence of SiC particles in the Al2014 alloy. As the SiC proportion grew from 5% to 10% wt., the density of the Al2014–SiC composites improved. The results showed that when the micro-SiC content in the Al2014 alloy increased, the ultimate, yield, and compression strength increased with a minimal drop in ductility. In an unreinforced material, fractured surfaces showed ductile mode fracture. Furthermore, as the reinforcing concentration increased to 10%, the composites began to shatter in a brittle manner.

Data Availability

No data were used to support this study.

Conflicts of Interest

The authors declare that they have no conflicts of interest.

References

[1] M. Song and Y. H. He, "Effects of die-pressing pressure and extrusion on the microstructures and mechanical properties of SiC reinforced pure aluminum composites," *Materials & Design*, vol. 31, no. 2, pp. 985–989, 2010.

[2] L Zhang, Q. wang, G. Liu, W. Guo, H. Jiang, and W. Ding, "Effect of SiC particles and the particulate size on the hot deformation and processing map of AZ91 magnesium matrix composites," *Materials Science and Engineering A*, vol. 707, pp. 315–324, 2017.

[3] S. A. Sajjadi, H. R. Ezatpour, and M. Torabi Parizi, "Comparison of microstructure and mechanical properties of A356 aluminium alloy/Al_2O_3 composites fabricated by stir and compo-casting process," *Materials & Design*, vol. 34, pp. 106–111, 2012.

[4] L. J. Zhang, D. L. Yang, F. Qiu, J. G. Wang, and Q. C. Jiang, "Effects of reinforcement surface modification on the microstructures and tensile properties of SiCp/Al2014 composites," *Materials Science and Engineering A*, vol. 624, pp. 102–109, 2015.

[5] W. Liao, B. Ye, L Zhang et al., "Microstructure evolution and mechanical properties of SiC nanoparticles reinforced magnesium matrix composite processed by cyclic closed die forging," *Materials Science and Engineering A*, vol. 642, pp. 49–56, 2015.

[6] X. J. Wang, N. Z. Wang, L. Y. Wang et al., "Processing, microstructure and mechanical properties of micro SiC particles reinforced magnesium matrix composites fabricated by stir casting assisted by ultrasonic treatment processing," *Materials & Design*, vol. 57, pp. 638–645, 2014.

[7] A. Baradeswaran and A. Elaya Perumal, "Study on mechanical and wear properties of Al7075-Al_2O_3-graphite hybrid composites," *Composites Part B: Engineering*, vol. 56, pp. 464–471, 2014.

[8] M. Ali and S. Mohsen Ostad, "Microstructural and abrasive wear properties of SiC reinforced aluminium based composite produced by compocasting," *Transactions of Nonferrous Metals Society of China*, vol. 23, pp. 1905–1914, 2013.

[9] K. Umanath, S. T. Selvamani, K. Palanikumar, T. Raphael, and K. Prashanth, "Effect of sliding distance on dry sliding wear behavior of Al6061-SiC-Al_2O_3 hybrid composite," in *Proceedings of the International Conference on Advances in Mechanical Engineering*, pp. 749–775, Bangkok, Thailand, April 2013.

[10] M. L. Ted Guo and C. Y. A. Tsao, "Tribological behavior of aluminum/SiC/nickel-coated graphite hybrid composites," *Materials Science and Engineering A*, vol. 333, no. 1-2, pp. 134–145, 2002.

[11] K. Yoganandam, K. Raja, and K. Lingadurai, "Mechanical and microstructural characterization of Al6082-TiO_2 metal matrix composites produced via compo casting method," *Indian Journal of Science and Technology*, vol. 9, no. 41, pp. 1–4, 2016.

[12] G. B. V. Kumar, C. S. P. Rao, N. Selvaraj, and M. S. Bhagyashekar, "Studies on Al6061-SiC and Al7075-Al_2O_3 metal matrix composites," *Journal of Minerals and Materials Characterization and Engineering*, vol. 9, no. 1, pp. 43–55, 2010.

[13] H. R. Ezatpour, M. Torabi-Parizi, and S. A. Sajjadi, "Microstructural and mechanical properties of extruded Al-Al_2O_3 composites fabricated by stir casting process," *Transactions of Nonferrous Metals Society of China*, vol. 23, no. 5, pp. 1262–1268, 2013.

[14] W. Wu, K. C. Goretta, and J. Routbort, "Erosion of 2014 Al reinforced with SiC or Al_2O_3 particles," *Materials Science and Engineering A*, vol. 151, no. 1, pp. 85–95, 1992.

[15] S. Suresh, N. Shenbaga Vinayaga Moorthi, S. C. Vettivel, and N. Selvakumar, "Mechanical behavior and wear prediction of stir cast Al-TiB_2 composites using response surface methodology," *Materials & Design*, vol. 59, pp. 383–396, 2014.

[16] P. Gurusamy and S. Balasivanandha Prabhu, "Influence of the squeeze pressure on the squeeze cast Al-SiCp metal matrix composites," *International Journal of Applied Engineering Research*, vol. 10, no. 71, pp. 365–370, 2015.

[17] H. Khosravi, H. Bakhshi, and E. Salahinejad, "Effects of compocasting process parameters on microstructural characteristics and tensile properties of A356–SiCp composites," *Transactions of Nonferrous Metals Society of China*, vol. 24, no. 8, pp. 2482–2488, 2014.

[18] B. Sirahbizu Yigezu, M. M. Mahapatra, and P. K. Jha, "Influence of reinforcement type on microstructure, hardness, and tensile properties of an aluminum alloy metal matrix composite," *Journal of Minerals and Materials Characterization and Engineering*, vol. 01, no. 04, pp. 124–130, 2013.

[19] J. David Raja Selvam, I. Dinaharan, S. Vibin Philip, and P. M. Mashinini, "Microstructure and mechanical characterization of in situ synthesized AA6061-TiB_2+Al_2O_3 hybrid aluminium matrix composites," *Journal of Alloys and Compounds*, vol. 740, pp. 529–535, 2018.

[20] C. Hu, H. Yan, J Chen, and B. Su, "Microstructures and mechanical properties of 2024Al/Gr/SiC hybrid composites fabricated by vacuum hot pressing," *Transactions of Nonferrous Metals Society of China*, vol. 26, no. 5, pp. 1259–1268, 2016.

[21] Y. H. Seo and C. Kang, "Effects of hot extrusion through a curved die on the mechanical properties of SiCp/Al composites fabricated by melt-stirring," *Composites Science and Technology*, vol. 59, no. 5, pp. 643–654, 1999.

[22] S. Naher, D. Brabazon, and L. Looney, "Development and assessment of a new quick quench stir caster design for the production of metal matrix composites," *Journal of Materials Processing Technology*, vol. 166, no. 3, pp. 430–439, 2005.

[23] K. Ravikumar, K. Kiran, and V. S. Sreebalaji, "Characterization of mechanical properties of aluminium-tungsten carbide composites," *Measurement*, vol. 102, pp. 142–149, 2017.

[24] T. Rajmohan, K. Palanikumar, and S. Ranganathan, "Evaluation of mechanical and wear properties of hybrid aluminium matrix composites," *Transactions of Nonferrous Metals Society of China*, vol. 23, no. 9, pp. 2509–2517, 2013.

[25] G. V. Kumar, A. R. K. Swamy, and A. Ramesha, "Studies on properties of as-cast Al6061-WC-Gr hybrid MMCs," *Journal of Composite Materials*, vol. 46, no. 17, pp. 2111–2122, 2011.

[26] N. Verma and S. C. Vettivel, "Characterization and experimental analysis of boron carbide and rice husk ash reinforced AA7075 aluminium alloy hybrid composite," *Journal of Alloys and Compounds*, vol. 741, pp. 981–998, 2018.

[27] N. Muralidharan, K. Chokalingam, I. Dinaharan, and K. Kalaiselvan, "Microstructure and mechanical behavior of AA2024 aluminium matrix composites reinforced with in situ

synthesized ZrB_2 particles," *Journal of Alloys and Compounds*, vol. 735, pp. 2467–2174, 2017.

[28] G. L. Rajesh, P. Badiger, V. Hiremath, V. Auradi, and S. A. Kori, "Investigation on mechanical properties of B_4C particulate reinforced Al6061 metal matrix composites," *International Journal of Applied Engineering Research*, vol. 10, no. 71, pp. 494–497, 2015.

[29] H. R. Ezatpour, S. A. Sajjadi, M. H. Sabzevar, and Y. Z. Huang, "An investigation of the tensile and compressive properties of Al6061 and its nanocomposites in as-cast state and in extruded condition," *Materials Science and Engineering A*, vol. 607, pp. 589–595, 2014.

[30] P. Mohan, M. Kathirvel, N. Azhagesan, and M. Sivapragash, "The mechanical characterization of Al_2O_3 reinforced Al6061 metal matrix composite," *Applied Mechanics and Materials*, vol. 766-767, pp. 257–262, 2015.

[31] S. Rajanna, "Evaluation of mechanical response of graphite reinforced metal matrix composite," *Journal of Harmonized Research*, vol. 1, no. 1, pp. 39–44, 2013.

[32] U. K. Annigeri and G. B. Veereshkumar, "Effect of reinforcement on density, hardness and wear behavior of aluminum metal matrix composites: a review," *Materials Today Proceedings*, vol. 5, no. 5, pp. 11233–11237, 2018.

[33] T. Lokesh and U. S. Mallik, "Dry sliding wear behavior of Al-Gr-SiC hybrid metal matrix composites by Taguchi techniques," *Materials Today Proceedings*, vol. 4, no. 10, pp. 11175–11180, 2017.

[34] M. Hossein Zadeh, O. Mirzaee, and P. Saidi, "Structural and mechanical characterization of Al based reinforced with heat treated Al_2O_3 particles," *Materials and Design*, vol. 54, pp. 245–250, 2014.